# Mathematic Model and Simulation of Magnetic Fluid Differential Transformer Tilt Sensor

**ABSTRACT**

A mathematical model of a mutual inductance magnetic fluid dip sensor is established, and its output characteristics are analyzed by simulation. The results show that the variable resistance of the measuring circuit can eliminate the residual zero voltage, and the output voltage carrier is positive half cycle after filtering and rectification. The addition of pure iron makes the mutual inductance change between primary and secondary windings greatly increase, and the inclination Angle has a linear relationship with the mutual inductance change in a small range. The recovery force on the composite core is proportional to the displacement.

*Keywords: magnetic fluid; sensor; simulation; Composite Core; measuring circuit; restoring force*

## 1.INTRODUCTION

The inclination sensor is a kind of component that converts the angle change of the input measured object into the output electrical signal, and is widely used in the technical fields of aerospace, transportation, industrial machinery, inertial navigation, etc.[1]. At present, the main development trend of sensor technology is to develop towards integration and intelligence, and to develop new materials and processes for sensors[2]. As a new functional material with both the magnetism of solid magnetic materials and the fluidity of liquid [3], magnetic fluid can be used as a sensitive element of sensors and has received great attention from researchers. The application of magnetic fluid has been studied earlier abroad. Magnetic fluid sensors are mostly used in military products, and the relevant literature reports are very few. It can be seen from the available literature that the United States, Romania, Japan, Russia and other countries have relatively mature research on the application of magnetic fluid in the field of sensors [4-9].

In recent years, China has carried out research in the application fields of magnetic fluid seals, sensors, shock absorbers, lubrication, etc. Professor Li Decai's team has carried out more systematic research on magnetic fluid sensors, and designed sensors based on the acceleration, inclination, micro-pressure difference and other types of magnetic fluid [10-16]. The magnetic fluid sensor has the advantages of shock resistance, high reliability, high sensitivity, and good low-frequency response. Based on this, a differential transformer type magnetic fluid inclination sensor is proposed in this paper. Combined with the differential rectification circuit, the zero residual voltage of the differential sensor can be eliminated, and the rationality of the design can be verified by simulation.

## 2.STRUCTURAL DESIGN AND WORKING PRINCIPLE

Fig.1 is the structural diagram of the magnetic fluid transformer type inclination sensor, which consists of: primary winding 1,2, secondary winding 3,4, E-39D epoxy resin 5, transparent acrylic tube 6, end cap 7, sealing ring 8, pure iron 9, permanent magnet ring 10, magnetic fluid 11.

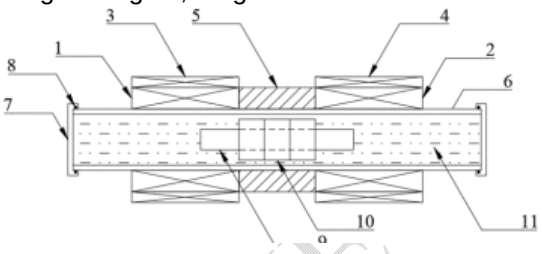


**Fig.1.Structural diagram of inclination sensor**

According to GB/T6109-2008, the diameter of enameled wire is 0.21mm and the number of turns of primary winding is 2000; The number of turns of secondary winding is 1000. E-39D epoxy resin has good electrical insulation performance and is often used to cast small transformers, where it is used to shield the mutual inductance of two primary windings. The oil-based magnetic fluid with model MF01 is initially selected, with saturation magnetization of 450 ± 50GS, density of 1.23kg/m$^3$ and viscosity of 20cp. The dimension parameters of each component of the inclination sensor are shown in Tab.1.

**Table.1.Dimensional parameters of each component of inclination sensor**

| | external diameter/ mm | internal diameter/ mm | length/ mm |
|---|---|---|---|
| primary winding | 20.4 | 12 | 21 |
| secondary winding | 24.6 | 20.4 | 21 |
| epoxy resin | 20.4 | 12 | 15 |
| acrylic tube | 12 | 10 | 80 |

| | | | |
|---|---|---|---|
| permanent magnet ring | 8 | 4 | 15 |
| pure iron | 4 | - | 30 |

The sensor is similar to the working principle of transformer. The movement of the composite core affects the mutual inductance of the primary and secondary windings. The size and parameters of the two primary windings are identical, and the same direction serial connection of the synonymous end is used as the excitation of the differential transformer type sensor, which is equivalent to the primary side of the transformer; The homonymous ends of the two secondary windings are inversely connected in series and output in differential mode, which is equivalent to the secondary side of the transformer. Therefore, the sensor is called a magnetic fluid differential transformer type tilt sensor. According to the second-order buoyancy principle of magnetic fluid, the permanent magnet ring is suspended in the center of the tube axis, and the magnetizing direction is along the axis. Adding pure iron bar can increase the relative permeability of the magnetic core, thus increasing the mutual inductance between the primary and secondary windings. When the sensor is in the horizontal state, the composite magnetic core is located in the center of the tube body, the mutual inductance $M_l$ between the primary and secondary windings at the left end=the mutual inductance $M_r$ between the primary and secondary windings at the right end, the mutual inductance electromotive force $U_l=U_r$, and the output differential pressure $\Delta U=U_l-U_r=0$; When the sensor is tilted, the composite magnetic core in the shell deviates from the balance position under the action of gravity and moves downward along the inclined tube wall, $M_l \neq M_r$, and the mutual inductance electromotive force $U_l \neq U_r$, that is, the output differential pressure $\Delta U=U_l-U_r \neq 0$. Each measured angle $\theta$ There is corresponding differential pressure $\Delta U$, and the measured angle can be obtained by measuring the differential pressure $\Delta U$ $\theta$ Value. The friction mode between the composite magnetic core and the tube wall is fluid friction, which is sensitive and has high measurement accuracy.

## 3.MATHEMATICAL MODEL CALCULATION

There are three kinds of media in the solenoid winding of the sensor, which are magnetic fluid, permanent magnet and pure iron. The magnetic fluid fills the whole inner cavity of the shell. The relative permeability of the magnetic fluid is approximately air. Assuming that the permanent magnet is fully magnetized to the saturation state, its relative permeability is close to air. Therefore, the medium in the coil can be equivalent to two parts, namely air and cylindrical iron core.

According to electromagnetism, the magnetic induction strength of solenoid winding with iron core consists of two parts:

### 3.1 Excitation magnetic induction intensity

Excitation magnetic induction intensity $B_l$ established by excitation current I in primary winding (winding magnetic field with magnetic fluid as medium);

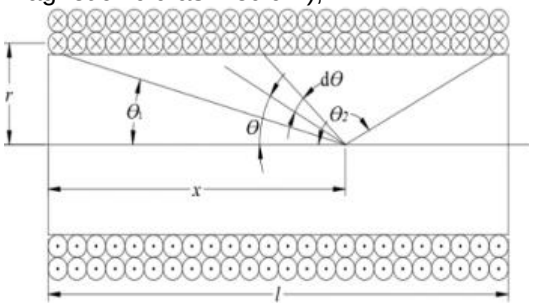


**Fig.2.Calculation of axial magnetic field distribution of solenoid winding**

According to Biot-Sapphire law, the magnetic induction intensity produced by the solenoid winding in the axial direction can be obtained.

$$B_l = \frac{\mu_0 NI}{2l}\left(\cos\theta_1 - \cos\theta_2\right) \qquad (1)$$

Where $N$ is the number of winding turns, $l$ is the length of solenoid winding, $r$ is the

average radius of solenoid winding, $\theta_1$,$\theta_2$respectively $\theta$ The value of angle at both ends of solenoid can be seen from Fig.2 $\theta_1$, cos $\theta_2$. The relationship with the field point coordinate $x$ is

$$\cos\theta_1 = \frac{x}{\sqrt{x^2 + r^2}} \quad (2)$$

$$\cos\theta_2 = -\frac{l - x}{\sqrt{(l - x)^2 + r^2}} \quad (3)$$

### 3.2 Additional magnetic induction strength

The additional magnetic induction intensity $B_a$ caused by the magnetization of pure iron after it enters the winding.

Pure iron is ferromagnetic material. When it enters the solenoid winding, the excitation magnetic field will magnetize it, and then generate additional magnetic field. This is replaced by the magnetic field generated by a circular current winding on the surface of pure iron.

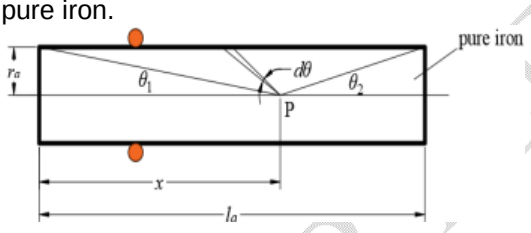


**Fig.3.Calculation of axial magnetic field distribution caused by pure iron magnetization**

Additional magnetic induction strength:

$$B_a = \int_0^{l_a} dB_a = \frac{\mu_0}{2} j(\cos\theta_1 - \cos\theta_2) \quad (4)$$

$j$—Is the ring current per unit length on the imaginary surface

Magnetization intensity M of an object at a certain point on pure iron M=$\chi_m$H,$\chi_m$ is the magnetic susceptibility of pure iron material, and $M$ is numerically equal to the circular current per unit length surrounding the point, that is, $j$=$M$.

$$\cos\theta_1 = \frac{x}{\sqrt{r_a^2 + x^2}} \quad (5)$$

$$\cos\theta_2 = -\frac{l_a - x}{\sqrt{(l_a - x)^2 + r_a^2}} \quad (6)$$

There are

$$B_a = \frac{\mu_0 \chi_m H}{2}\left(\frac{x}{\sqrt{r_a^2 + x^2}} + \frac{l_a - x}{\sqrt{(l_a - x)^2 + r_a^2}}\right) \quad (7)$$

By electromagnetism:

$$B_l = \mu_0(H + M) = \mu_0(1 + \chi_m)H \quad (8)$$

$$\mu_r = 1 + \chi_m \quad (9)$$

So

$$B_l = \mu_0 \mu_r H \quad (10)$$

Introduction of equivalent permeability $\mu_e$:

$$\mu_e = \frac{\chi_m}{\mu_r} \quad (11)$$

$$\mu_0 \chi_m H = \mu_0 \mu_r H \mu_e \quad (12)$$

The above formula becomes

$$B_a = \frac{\mu_e B_l}{2}\left(\frac{x}{\sqrt{r_a^2 + x^2}} + \frac{l_a - x}{\sqrt{(l_a - x)^2 + r_a^2}}\right) \quad (13)$$

### 3.3 Total magnetic induction intensity

Total magnetic induction intensity of solenoid winding with pure iron=excitation magnetic induction intensity of winding+ additional magnetic induction intensity of pure iron magnetization

$$B = B_l + B_a = \frac{\mu_0 NI}{2l}\left[\frac{x}{\sqrt{x^2 + r^2}} + \frac{l - x}{\sqrt{(l - x)^2 + r^2}}\right] + \frac{\mu_e B_l}{2}\left[\frac{x}{\sqrt{r_a^2 + x^2}} + \frac{l_a - x}{\sqrt{(l_a - x)^2 + r_a^2}}\right] \quad (14)$$

Total magnetic flux:

$$\Phi = \Phi_l + \Phi_a = B_l A_l + B_a A_a = B_l \pi R^2 + B_a \pi r_a^2 \quad (15)$$

$$\Psi = \Psi_l + \Psi_a = \Phi_l N + \Phi_a N_a = \int_0^l \Phi_l n dx + \int_0^{l_a} \Phi_a n dx \quad (16)$$

Known $L = \frac{\Psi}{I}$, $\Psi$- flux linkage, $I$- Excitation current

$$\Psi_l = \int_0^l B_l A_l n dx = \int_0^l \frac{\mu_0 In}{2}[f(x)] A_l \, n dx = In^2 \mu_0 \pi r^2 \left(\sqrt{l^2 + r^2} - r\right) \quad (17)$$

$$\Psi_a = \int_0^{l_a} \frac{\mu_e B_l}{2}[g(x)]A_a n dx$$
$$= \frac{\mu_e}{2} \cdot \frac{\mu_0 l n^2}{2} A_a \int_0^{l_a} [f(x)][g(x)]dx \quad (18)$$
$$= \frac{l n^2 \mu_0 \mu_e \pi r^2}{2}\left(\sqrt{l_a^{\,2} + r_a^{\,2}} - r_a\right)$$

$$\Psi_{11} = \Psi_l + \Psi_a = l n^2 \mu_0 \pi \left[ r^2 \left(\sqrt{l^2 + r^2} - r\right) + \frac{\mu_e r_a^2}{2}\left(\sqrt{l_a^{\,2} + r_a^{\,2}} - r_a\right)\right] \quad (19)$$

The self-induction of primary winding $W_1$ is

$$L_1 = \frac{\Psi_{11}}{l} = n^2 \mu_0 \pi \left[ r^2 \left(\sqrt{l^2 + r^2} - r\right) + \frac{\mu_e r_a^2}{2}\left(\sqrt{l_a^2 + r_a^2} - r_a\right)\right] \quad (20)$$

The secondary winding $W_3$ is tightly wound on the outside of the primary winding $W_1$, so if the magnetic flux of the primary winding $W_1$ enters the secondary winding $W_3$

$$\Psi_{13} = \Psi_{11} = l n^2 \mu_0 \pi \left[ r^2 \left(\sqrt{l^2 + r^2} - r\right) + \frac{\mu_e r_a^2}{2}\left(\sqrt{l_a^{\,2} + r_a^{\,2}} - r_a\right)\right] \quad (21)$$

Therefore, the mutual inductance coefficient $M_l$ between primary winding $W_1$ and secondary winding $W_3$ on the left side is

$$M_l = M_{31} = M_{13} = \frac{\Psi_{13}}{l} = n^2 \mu_0 \pi \left[ r^2 \left(\sqrt{l^2 + r^2} - r\right) + \frac{\mu_e r_a^2}{2}\left(\sqrt{l_a^2 + r_a^2} - r_a\right)\right] \quad (22)$$

At the beginning, the composite magnetic core is in the middle position. Under the condition of strict technology, the two windings can be symmetrical, that is, $N_1$=$N_2$, $N_3$=$N_4$, $L_1$=$L_2$. At this time, the mutual inductance coefficient $M_r$ between the right primary winding $W_2$ and the secondary winding $W_4$ is

$$M_r = M_l = n^2 \mu_0 \pi \left[ r^2 \left(\sqrt{l^2 + r^2} - r\right) + \frac{\mu_e r_a^2}{2}\left(\sqrt{l_a^2 + r_a^2} - r_a\right)\right] \quad (23)$$

The output induced electromotive force is zero.

When the sensor is tilted, the composite magnetic core moves to the left $\Delta x$, and the mutual inductance of the left and right sides can be expressed as

$$M_l' = n^2 \mu_0 \pi \left[ r^2 \left(\sqrt{(l - \Delta x)^2 + r^2} - r\right) + \frac{\mu_e r_a^2}{2}\left(\sqrt{(l_a + \Delta x) + r_a^2} - r_a\right)\right] \quad (24)$$

$$M_r' = n^2 \mu_0 \pi \left[ r^2 \left(\sqrt{(l + \Delta x)^2 + r^2} - r\right) + \frac{\mu_e r_a^2}{2}\left(\sqrt{(l_a - \Delta x) + r_a^2} - r_a\right)\right] \quad (25)$$

Assuming that the length of the solenoid is $l \gg$ radius $r$, the magnetic field is nearly uniform within a large range of the solenoid, the length of the iron core is $l_a \gg$ radius $r_a$, and the epoxy resin material between the left and right primary windings shields the mutual inductance of the two primary windings, ignoring $r$ and $r_a$, we can get:

$$\Delta M = M_l' - M_r' = n^2 \mu_0 \pi \Delta x \left(r_a^2 \mu_e - 2r^2\right) = n^2 \mu_0 \pi \frac{mg}{k}\left(r_a^2 \mu_e - 2r^2\right)\sin\theta \quad (26)$$

When measuring in small angle range

$$\Delta M = n^2 \mu_0 \pi \frac{mg}{k}\left(r_a^2 \mu_e - 2r^2\right)\theta \quad (27)$$

The angle change is approximately linear with the mutual inductance change of primary and secondary windings, and the sensitivity of this sensor is

$$S = \frac{\Delta M}{\theta} = n^2 \mu_0 \pi \frac{mg}{k}\left(r_a^2 \mu_e - 2r^2\right) \quad (28)$$

Where $n$=$N$/$l$, is the number of winding turns per unit length, and $k$ is the slope of the restoring force versus displacement curve. It can be seen from Equation 28 that to improve the sensitivity of the sensor, increase the number of winding turns, increase the cross-sectional area of the iron core, and select high permeability materials to increase $\mu_e$.

## 4.SIMULATION MODELING AND RESULT ANALYSIS

The magnetic field excitation source of the inclination sensor consists of two parts, one is the constant magnetic field generated by the permanent magnet ring, and the other is the alternating magnetic field generated by the alte'nating current as the excitation source. The permanent magnet ring is set to move in the pipe, and the model is completely symmetrical about the central

axis of the pipe body, and 360° rotation around the axis is the 3D model. In order to reduce the calculation amount and save the solution time, the 2D transient field solver is selected, and the geometric model is symmetrical about the z axis; In the ANSYS Maxwell preprocessor, the structural model of the magnetic fluid transformer type tilt sensor is established.

After the structural model is established, define the material of each component, set the magnetizing direction of the permanent magnet ring to be the positive direction of the z axis, and the magnetic property of the magnetic fluid is the key parameter of the change of the magnetic fluid inclination sensor sensing signal[4], so set the relative permeability of the magnetic fluid to be slightly greater than the relative permeability of the air, and its value is 1.25; The conductor model is selected as Stranded, which is used to simulate the current carried by the wound conductor. Eddy current effect is not considered in the calculation; Set the air domain region=100%, and apply the vector magnetic potential boundary condition $A_z$=0 to the air domain, that is, the magnetic field line is parallel to the air domain boundary, the air domain grid is divided into 3mm, and the model grid is 0.5mm. Solve after checking that there is no error, and the magnetic field line distribution is analyzed as shown in Fig.4.

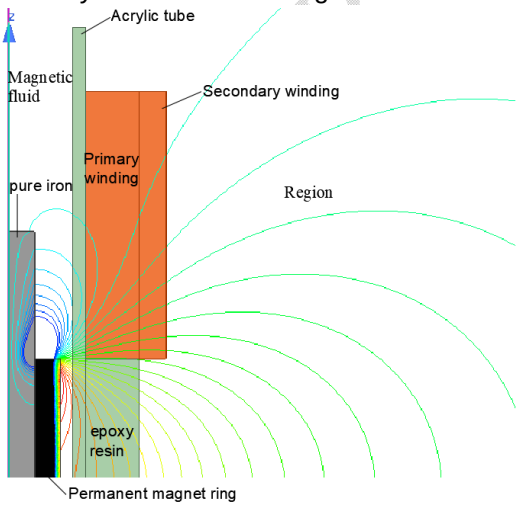


**Fig.4.Distribution of magnetic lines of force**

Set the winding excitation as an external circuit, and establish the external circuit model in Twin Builder. The input peak value of the primary winding is 3V sine AC voltage signal, the frequency is 500Hz, and the solution time is 5 cycles, a total of 10ms. The excitation voltage waveform of the primary winding $W_1$ is obtained as shown in Fig.5.

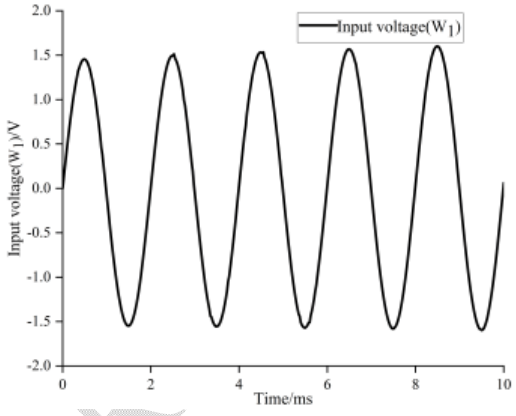


**Fig.5. Excitation voltage waveform of primary winding $W_1$**

The external circuit is shown in Fig.6, which is the measuring circuit of the transformer type tilt sensor. The two secondary output voltages of the sensor are rectified separately, and then the rectified voltage difference is used as the output. The variable resistance $R_0$ in the Fig. is used to adjust the zero residual voltage.

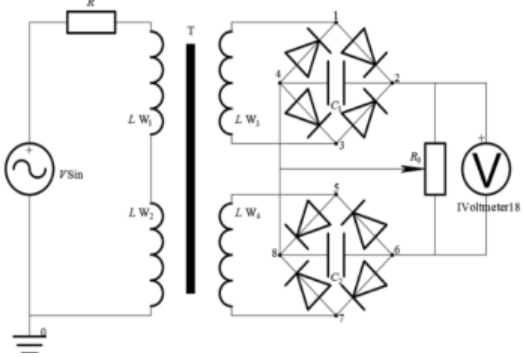


**Fig.6.External circuit**

As shown in Fig.7, the sensor output voltage is 0 when the composite core is at the initial position. The measuring circuit is full-wave voltage output type.

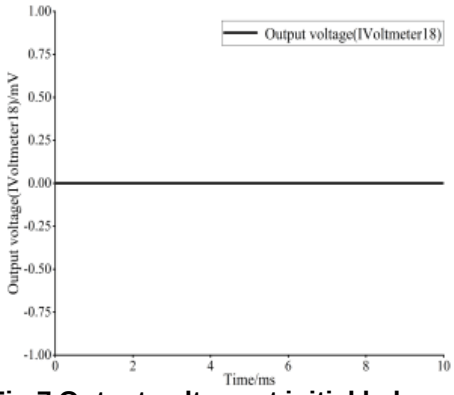


**Fig.7.Output voltage at initial balance position**

## 4.1 Output voltage analysis

When the inclination sensor is tilted, the composite magnetic core deviates from the balance position along the axis of the tube body under the action of gravity, and the angle tilt is converted into the translational movement of the composite magnetic core. The inner cavity of the tube body is set as the moving area. The moving object is the composite magnetic core suspended in the magnetic fluid, moving forward along the z axis for 1 mm, with a speed of 100 mm/s. The results show that the maximum output voltage is 119.48mV, and the potential difference between the two ends of the secondary winding $W_3$ is greater than the potential difference between the two ends of $W_4$, The voltage difference $U_{24}$ at both ends of capacitor $C_1$ is greater than the voltage difference $U_{68}$ at both ends of capacitor $C_2$. The voltage carrier after filtering and rectification is positive half cycle, as shown in Fig.8.

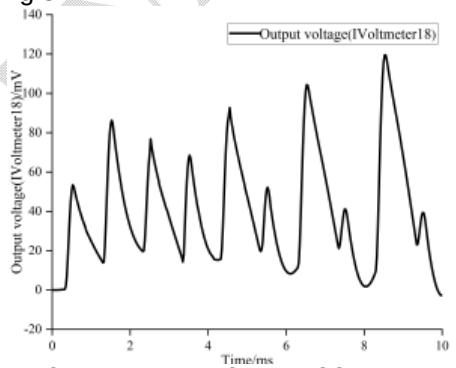


**Fig.8.Output voltage with 1mm movement**

Parameterized setting of composite core movement is 1mm,2mm,3mm and 4mm, corresponding to the increasing tilt angle. It can be seen from Fig.9 that the output voltage increases in turn with the increase of composite core movement distance.

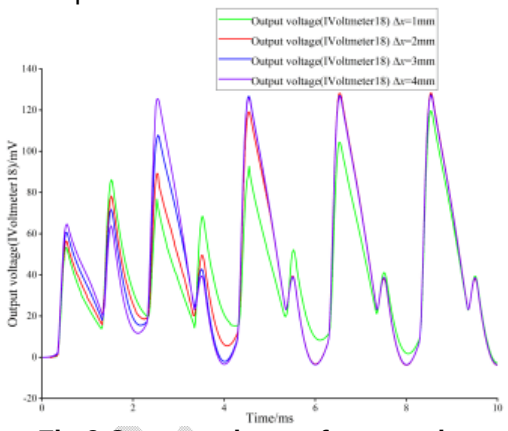


**Fig.9.Output voltage of composite magnetic core at different positions**

## 4.2 Inductance variation of different cores

Fig.10 shows the mutual inductance change between primary winding $W_1$ and secondary winding $W_3$ of the sensor when the permanent magnet with a diameter of 8mm and a length of 30mm moves forward along the z axis from the balance position. The inductance matrix is set as the apparent inductance. The results show that the incremental curve is basically linear, the mutual inductance at the balance position is 32.163mH, and the mutual inductance increment is 0.078mH after the magnetic core moves 1mm.

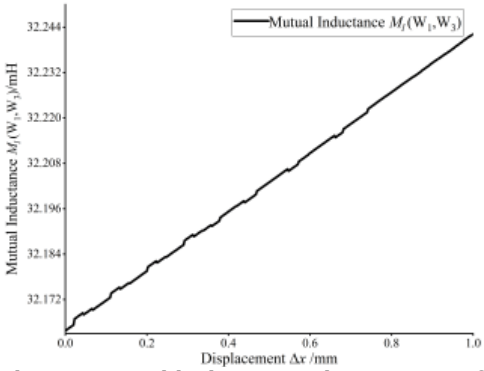


**Fig.10.Mutual inductance increment of primary and secondary windings of permanent magnet with magnetic core**

Fig.11 shows the mutual inductance change between primary winding $W_1$ and secondary winding $W_3$ of the sensor when the composite core added with pure iron moves forward 1mm along the z axis from the balance position. The incremental curve is linear, and the slope is the sensitivity of the sensor. The mutual inductance at the balance position is 54.978mH, and the mutual inductance increment is 3.85mH after the composite core moves 1mm.

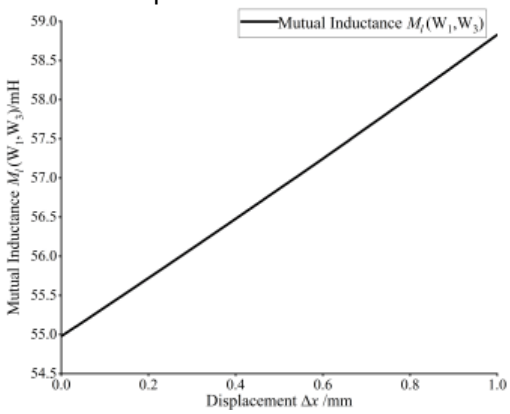


**Fig.11.Mutual inductance increment of primary and secondary windings with composite core**

## 4.3 Recovery force simulation

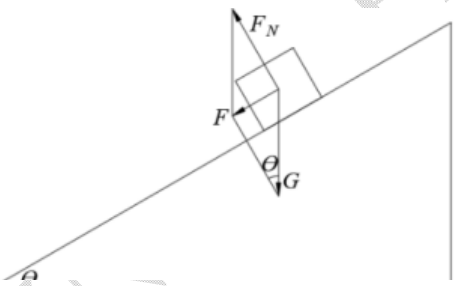


**Fig.12.Stress analysis diagram of composite magnetic core**

When the sensor is tilted, the internal composite magnetic core produces a downward component force along the pipe wall under the action of gravity $F=mg\sin\theta$,The mass of the composite core is m=7.24g, and its recovery force is composed of two parts: the second-order buoyancy force of the magnetic fluid $F_m$ and the ampere force $F_a=N_0BIL$ generated by the permanent magnet ring in the solenoid. When $F_m+F_a=F$ is met, the composite core reaches balance at a certain position. With the increase of the tilt angle, $F$ increases, the effective number of turns $N_0$ through the permanent magnet ring increases, that is, $F_a$ increases, and the composite core reaches a new balance in the process of movement. Compared with the existing magnetic fluid sensors, permanent magnets are installed at both ends of the shell to provide the restoring force, which simplifies the structure and improves the measuring range.

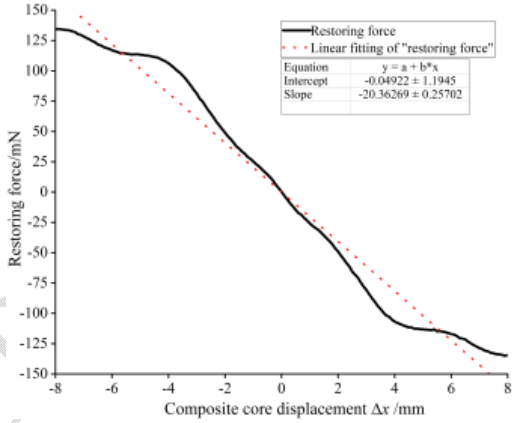


**Fig.13.Relation between recovery force and displacement of composite magnetic core**

In the parameters option, apply a force condition to the composite core, and the composite core moves within ±8mm. The simulation results are shown in Fig.13. It can be seen from Fig.13 that the recovery force of the composite core is 0 at the initial position $\Delta x=0$. When the sensor is tilted, the composite core deviates from the initial position, and the recovery force is proportional to the displacement, and the linear area is large.

## CONCLUSION

(1) In this paper, a magnetic fluid differential transformer type tilt sensor based on mutual inductance principle is designed. Combined with full-wave voltage output type measuring circuit, the variable resistance is used to adjust the zero residual voltage of the differential tilt sensor. The output voltage

carrier after rectification and filtering is positive half cycle.

(2) The theoretical formula of the magnetic fluid differential transformer type inclination sensor is derived. It is concluded that the inclination change is linear with the mutual inductance change of the primary and secondary windings in a small range, and the slope is the sensitivity. The simulation results are consistent with the calculation results.

(3) The magnetic core structure of the magnetic fluid sensor based on the second-order buoyancy principle is improved, and pure iron is added to the permanent magnet ring. The simulation results show that the mutual inductance change of the sensor after adding pure iron is significantly higher than that of the sensor with a single permanent magnet.

(4) The simulation results show that the recovery force of the composite magnetic core is proportional to the displacement, and the structure is simpler without external magnets.

## REFERENCE:


1. Su Shuqiang, Li Decai. Research on magnetic fluid inclination sensor [J]. Journal of Metrology,2016,37(04):366-370.
2. Chen Jie, Huang Hong Sensor and detection technology. 2nd edition [M]. Higher Education Press, 2010.
3. Zhao Xinyuan, Zhang Fengxuan, Lu Ying, Su Bo. Research on magnetic fluid birefringence effect based on quartz glass microfluidic chip [J]. Technological innovation and application,2021,11(22):19-21.
4. Cui Hairong, Zheng Jinju, Yang Chaozhen, Wang Xuefeng. Numerical simulation and experimental verification of magnetic fluid level sensor [J]. China Mechanical Engineering,2012,23(20):2424-2429.
5. Cotae C , Baltag O , Olaru R , et al. The study of a magnetic fluid-based sensor[J]. Journal of Magnetism & Magnetic Materials, 1999, 201(1-3):394-397.
6. Piso M I . Applications of magnetic fluids for inertial sensors[J]. Journal of Magnetism & Magnetic Materials, 1999, 201(1-3):380-384.
7. Thilwind R E , Megens M , Zon J , et al. Measurement of the concentration of magnetic nanoparticles in a fluid using a giant magnetoresistance sensor with a trench[J]. Journal of Magnetism & Magnetic Materials, 2008, 320(3-4):486-489.
8. Ando B , Ascia A , Baglio S , et al. A Ferrofluidic Inertial Sensor Exploiting the Rosensweig Effect[J]. IEEE Transactions on Instrumentation and Measurement, 2010, 59(5):1471-1476.
9. G. Chitnis, B. Ziaie. A ferrofluid-based wireless pressure sensor[J]. Journal of Micromechanics and Microengineering, 2013, 23(12): 125031(6pp).
10. Dong Guoqiang, Li Decai, Hao Ruishen. Research on micro differential pressure sensor based on ferromagnetic fluid [J]. Journal of Sensing Technology,2009,22(01):50-53.
11. Hao Ruishen, Li Decai. Mathematical model calculation and experimental verification of differential magnetic fluid micro-pressure differential sensor [J]. Journal of Mechanical Engineering,2010,46(12):161-165.
12. Han Qi Application of magnetic fluid in inclination sensor [D]. Beijing Jiaotong University,2011.
13. Qian Leping, Li Decai. Theoretical and experimental research on a new magnetic liquid inertial sensor [J]. Journal of Instrumentation,2015,36(3):507-514.
14. Xie Jun, Li Decai, Xing Yansi. Design and withstand voltage analysis of a new type of magnetic fluid micro-pressure differential sensor [J]. Journal of Instrumentation,2015, 36(9): 2005-2012.
15. Wang Huan Theoretical and experimental research on magnetic fluid inclination sensor [D]. North University of Technology,2019.
16. Feng Zihang Research on a new magnetic fluid inclination sensor [D]. Beijing Jiaotong University,2020.